Combination of Novel Green Fluorescent Protein Mutant TSapphire and DsRed Variant mOrange to Set Up a Versatile in Planta FRET-FLIM Assay[1][W]

Vincent Bayle, Laurent Nussaume, and Riyaz A. Bhat[2]*

Laboratory of Plant Developmental Biology, Service of Plant Biology and Environmental Microbiology/ Institute for Biotechnology and Environmental Biology, UMR6191 CEA/CNRS/Mediterranean University Aix-Marseille, CEN, Cadarache, 13108 St. Paul Lez Durance, France

Förster resonance energy transfer (FRET) measurements based on fluorescence lifetime imaging microscopy (FLIM) are increasingly being used to assess molecular conformations and associations in living systems. Reduction in the excited-state lifetime of the donor fluorophore in the presence of an appropriately positioned acceptor is taken as strong evidence of FRET. Traditionally, cyan fluorescent protein has been widely used as a donor fluorophore in FRET experiments. However, given its photolabile nature, low quantum yield, and multiexponential lifetime, cyan fluorescent protein is far from an ideal donor in FRET imaging. Here, we report the application and use of the TSapphire mutant of green fluorescent protein as an efficient donor to mOrange in FLIM-based FRET imaging in intact plant cells. Using time-correlated single photon counting-FLIM, we show that TSapphire expressed in living plant cells decays with lifetime of 2.93 ± 0.09 ns. Chimerically linked TSapphire and mOrange (with 16-amino acid linker in between) exhibit substantial energy transfer based on the reduction in the lifetime of TSapphire in the presence of the acceptor mOrange. Experiments performed with various genetically and/or biochemically known interacting plant proteins demonstrate the versatility of the FRET-FLIM system presented here in different subcellular compartments tested (cytosol, nucleus, and at plasma membrane). The better spectral overlap with red monomers, higher photostability, and monoexponential lifetime of TSapphire makes it an ideal FRET-FLIM donor to study protein-protein interactions in diverse eukaryotic systems overcoming, in particular, many technical challenges encountered (like autofluorescence of cell walls and fluorescence of pigments associated with photosynthetic apparatus) while studying plant protein dynamics and interactions.

Single- and dual-color fluorescence imaging with intrinsically fluorescent proteins is increasingly being used to study the expression, targeting, colocalization, turnover, and associations of diverse proteins involved in different plant signal transduction pathways (for review, see Fricker et al., 2006). Concurrent with the use of fluorescence-based cell biology, Förster resonance energy transfer (FRET) has emerged as a convenient tool to study the dynamics of protein associations in vivo. The technique exploits the biophysical phenomenon of nonradiative energy transfer from a donor fluorophore to an appropriately positioned acceptor at a nanometer scale (1–10 nm; Jares-Erijman and Jovin, 2003). In living cells, FRET occurs when two proteins (or different domains within a single protein) fused to suitable donor and acceptor fluorophores physically interact, thus bringing the donor and the acceptor within the favorable proximity for energy transfer (Immink et al., 2002; Bhat et al., 2006). This results in a decrease in the donor's fluorescence intensity (or quantum yield [QY]) and excited-state lifetime (Gadella et al., 1999). Furthermore, if the acceptor molecule is a fluorophore, then FRET additionally results in an increase in the acceptor's emission intensity (sensitized emission; Shah et al., 2001; Bhat et al., 2006).

However, the exploitation and use of fluorescent marker proteins to study protein trafficking and associations in plants can be problematic because plant cells contain a number of autofluorescent compounds (e.g. lignin, chlorophyll, phenols, etc.) whose emission spectra interfere with that of the most commonly used green or red fluorescent protein fluorophores and/or their spectral variants. For example, lignin fluorescence in roots, vascular tissues, and cell walls of aerial plant parts interferes with imaging at wavelengths between 490 and 620 nm, whereas the chlorophyll autofluorescence in green aerial plant parts is prevalent between 630 and 770 nm (Chapman et al., 2005). Consequently, conventional imaging of GFP and its closest spectral variants (like cyan fluorescent protein [CFP] and yellow fluorescent protein [YFP]) is most likely to be problematic in roots, whereas red-shifted intrinsic fluorescent proteins (including monomeric red fluorescent protein and recently identified spectral variants like mStrawberry and mCherry) may be hard to discriminate in chloroplast-containing aerial tissues (Chapman et al., 2005). The problems get further compounded in

[1] This work was supported by the French Atomic Energy Agency.

[2] Present address: Department of Biology, Indiana University, Bloomington, IN 47405.

* Corresponding author; e-mail bhatr@indiana.edu.

The author responsible for distribution of materials integral to the findings presented in this article in accordance with the policy described in the Instructions for Authors (www.plantphysiol.org) is: Riyaz A. Bhat (bhatr@indiana.edu).

[W] The online version of this article contains Web-only data.
www.plantphysiol.org/cgi/doi/10.1104/pp.108.117358

FRET assays because the autofluorescence arising from phenols, lignin, and chlorophyll can limit the choice of fluorophores suitable for in planta FRET assays.

CFP and YFP have been widely used as a donor-acceptor pair in in planta FRET measurements (Bhat et al., 2006; Dixit et al., 2006). However, in photophysical terms, this pair is less than ideal for FRET imaging. Both have broad excitation and emission spectra with a small Stokes shift (Chapman et al., 2005). Second, QY of CFP (QY = 0.4) is relatively lower than that of YFP (QY = 0.61), and thus a significantly higher (and rather cell damaging) amount of excitation energy is needed to induce FRET (Dixit et al., 2006). Additionally, CFP displays multiexponential lifetimes with a shorter (1.3 ns) and a longer (2.6 ns) component (Becker et al., 2006). Although the deviation from the single-component decay is reasonably small (Tramier et al., 2002; Becker et al., 2006), the shorter CFP lifetime component can erroneously be interpreted as being the result of lifetime reduction due to energy transfer. At the same time, weak or transient protein associations may get masked and thus remain undetected. Whereas the parental wild-type GFP is extremely photostable and shows a monoexponential decay pattern (excited-state lifetime 3.16 ± 0.03 ns; Striker et al., 1999; Volkmer et al., 2000; Shaner et al., 2005), its close spectral overlap with YFP makes it unsuitable as a donor in GFP-YFP FRET experiments. Likewise, wild-type or enhanced GFP (or YFP) as a donor to red-shifted monomers as acceptors is suboptimal because the 488-nm (or 514-nm) laser line commonly used to excite GFP (or YFP) cross excites most of the red monomers (e.g. mOrange, mStrawberry) because of their broad excitation spectra (Zapata-Hommer and Griesbeck, 2003; Shaner et al., 2004).

Recently, TSapphire (Q69M/C70P/V163A/S175G; excitation/emission 399/511 nm), a variant of the Sapphire (T203I) mutant of wild-type GFP with improved folding properties and better pH sensitivity, was described (Zapata-Hommer and Griesbeck, 2003). The T203I mutation in TSapphire (and original Sapphire as well) abolishes the 475-nm excitation peak found in the wild-type GFP (Tsien, 1998). TSapphire is efficiently excited below 410 nm, which makes it ideal for studying plant protein dynamics and interactions because, at this wavelength, there is negligible excitation of the autofluorescing chlorophyll pigments. Furthermore, TSapphire also represents a good donor to red monomer acceptors that are negligibly excited at this wavelength (Shaner et al., 2004). Using a purified Zn^{2+} sensor with TSapphire and mOrange as a donor-acceptor pair, Shaner and colleagues demonstrated the ratiometric intramolecular FRET between the two fluorophores in vitro (Shaner et al., 2004). The sensor yielded a 6-fold ratiometric increase (562/514-nm mOrange/TSapphire emission ratio) upon Zn^{2+} binding.

However, currently there are no reports demonstrating the application and use of TSapphire and monomeric red-shifted fluorophores as donor-acceptor FRET pairs to probe intermolecular protein-protein interactions in vivo. In this article, we demonstrate in vivo FRET-fluorescence lifetime imaging microscopy (FLIM) between the donor TSapphire and the acceptor mOrange. We show that TSapphire expressed in living plant cells decays with a monoexponential lifetime of 2.93 ± 0.09 ns, which is in agreement with the published lifetime for its parent wild-type GFP (3.2 ns; Striker et al., 1999; Volkmer et al., 2000). Furthermore, we demonstrate intramolecular FRET-FLIM between chimerically linked TSapphire and mOrange (with a 16-amino acid linker in between). When fused to genetically known interacting proteins and expressed in intact living cells, the donor and the acceptor fluorophores show energy transfer in different subcellular compartments indicative of intermolecular protein-protein interactions. These results validate the versatility of the proposed in vivo FRET-FLIM assay based on the donor TSapphire and the acceptor mOrange, which turns out to work with both soluble and membrane proteins.

RESULTS

Construction of p35S Binary Vectors for Expression of C-Terminally Fluorescently Tagged Proteins in Planta

Binary vectors based on the pam-PAT-MCS backbone (accession no. AY436765) were generated to allow convenient and rapid in planta expression of proteins with TSapphire and mOrange fluorescent tags (see "Materials and Methods" for cloning details). The resulting vectors are high copy number in *Escherichia coli* and confer ampicillin and carbenicillin resistance to *E. coli* and *Agrobacterium tumefaciens*, respectively. The *pat* gene confers Basta herbicide resistance, allowing rapid selection of transgenic plants on soil (Witte et al., 2004). The construct p35S::TSapphire-mOrange-nos expressing the chimeric TSapphire-mOrange protein separated by a 16-amino acid linker represents a crucial positive control to assess the general conditions for setting up in planta FRET-FLIM based on the two fluorophores.

Expression and Spectral Analysis of TSapphire, mOrange, and Chimeric TSapphire-mOrange Fluorophores in Intact Plant Cells

To examine the expression of TSapphire, mOrange, or TSapphire-mOrange chimeric fluorophores in intact living cells, transient gene expression studies were carried out by particle bombardment (Bhat et al., 2005) in detached *Nicotiana benthamiana* leaves. The leaves were bombarded with gold particles coated with equimolar amounts of p35S::TSapphire-nos and p35S::mOrange-nos or with p35S::TSapphire-mOrange-nos chimeric construct and analyzed by confocal laser scanning microscopy (CLSM) after incubation at room temperature for 18 to 24 h (Fig. 1, A–F). Figure 1, A to C, shows a representative image of a *N. benthamiana* cell coexpressing TSapphire (Fig. 1A) and mOrange (Fig. 1B) along with an overlay image (Fig. 1C) of the two fluorophores. From the combined overlay image, it is

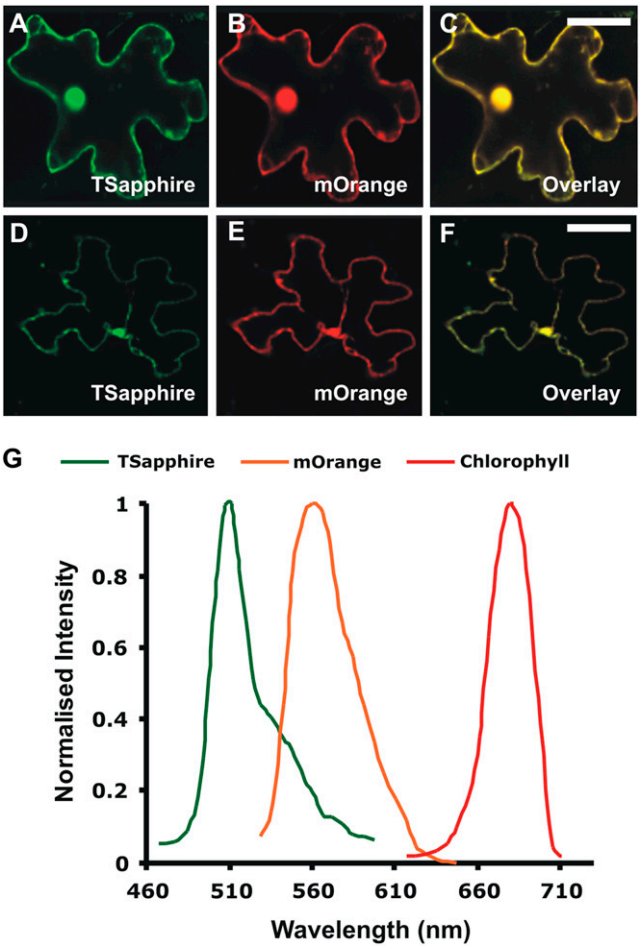

Figure 1. Coexpression of TSapphire and mOrange or chimeric TSapphire-mOrange in intact plant cells. A to C, Confocal images of a representative *N. benthamiana* leaf epidermal cell coexpressing TSapphire and mOrange. D to F, Confocal image of a representative *N. benthamiana* cell expressing the chimeric TSapphire-mOrange protein. A and D, TSapphire in green. B and E, mOrange in red. C and F, Overlay images of A and B and D and E, respectively. Scale bars = 45 μm. G, Emission spectra of the TSapphire and mOrange fluorophores expressed in *N. benthamiana* cells. Also shown is the emission spectrum of chlorophyll autofluorescence. Fluorescence emission spectra were recorded in a λ-spectral mode from 450 to 590 nm for TSapphire; 540 to 660 nm for mOrange; and 600 to 720 nm for chlorophyll using a Leica LCS SP2 CLSM.

clear that both fluorophores completely colocalize in the cytosol, as well as in the nucleus, as would be expected for soluble proteins without any specific localization signal. Imaging of the cells expressing the chimeric TSapphire-mOrange also gave similar results. Figure 1, D to F, shows the results of a representative cell expressing the TSapphire (Fig. 1D) and mOrange (Fig. 1E) from the chimeric construct along with an overlay image of the two fluorophores (Fig. 1F). Spectral analysis confirmed that the cells were expressing fluorophores with the correct emission spectra (Fig. 1G) and that the emission spectrum of mOrange showed hardly any overlap with the chlorophyll autofluorescence (Fig. 1G).

Excited-State Lifetime Analysis of TSapphire Expressed in *N. benthamiana* Leaves

N. benthamiana cells transiently expressing the TSapphire fluorophore were subjected to time-correlated single photon counting (TCSPC)-FLIM analysis to ascertain the excited-state lifetime of the fluorophore. Eighty-megahertz repetitive pulses from a 405-nm diode laser were used to excite the TSapphire and build up the photon decay profile over time (40 cycles of 6 s/cycle) as described in "Materials and Methods." The decay profile was built using a single exponential decay model. Figure 2 shows an overview of the lifetime image and the distribution profile along with fitted fluorescence decay at a single pixel (shown by an arrowhead in A) of a *N. benthamiana* cell expressing TSapphire. The lifetime image (Fig. 2A) and the overall lifetime distribution profile (Fig. 2B) represent the spatial distribution of the fluorescence lifetime in pseudocolor from red (2.1 ns) to blue (3.1 ns). From the lifetime distribution profile (Fig. 2B), it is quite clear that a majority of the photons decay around 3.0 ns. Figure 2C shows the fluorescence decay functions of a 3 $\times$ 3 pixel region around the red arrowhead location indicated in Figure 2A using a single exponential fit. The average lifetime of the TSapphire measured in three independent experiments was found to be 2.93 $\pm$ 0.09 ns (see Table I), which is in agreement with the published lifetime for its parent wild-type GFP (3.16 $\pm$ 0.03 ns; Volkmer et al., 2000).

FRET-FLIM Analysis in Cells Expressing Chimeric TSapphire-mOrange Fusion Protein

To examine the changes in the lifetime of the donor TSapphire in the presence of the acceptor mOrange, *N. benthamiana* cells expressing TSapphire and mOrange either from separate plasmids or from the chimeric construct harboring TSapphire and mOrange separated by 16-amino acid linker were used for FRET-FLIM as shown in Figure 3. Figure 3, A and C, shows the pseudocolored lifetime images of the donor TSapphire in representative cells either coexpressing both TSapphire and mOrange from separate plasmids or expressing a chimeric TSapphire-mOrange fusion from a single plasmid. Figure 3, B and D, represent the overall lifetime distribution of the photons depicted in Figure 3, A and C, respectively. As can be seen from Figure 3B, majority of the TSapphire photons show a longer lifetime above 2.9 ns. The averaged mean lifetime of TSapphire in cells coexpressing free TSapphire and free mOrange was found to be 2.87 $\pm$ 0.08 ns. Using the FRET-FLIM efficiency formula (see "Materials and Methods"), this amounts to an energy transfer of 2% (see Table I). On the other hand, lifetime analysis in cells expressing TSapphire-mOrange chimeric protein results in a significant shift in the lifetime profile of the donor (Fig. 3D). The mean lifetime of TSapphire in cells expressing chimeric protein was found to be 2.48 $\pm$ 0.04 ns amounting to 15% energy transfer from the donor TSapphire to the acceptor mOrange (Table I).

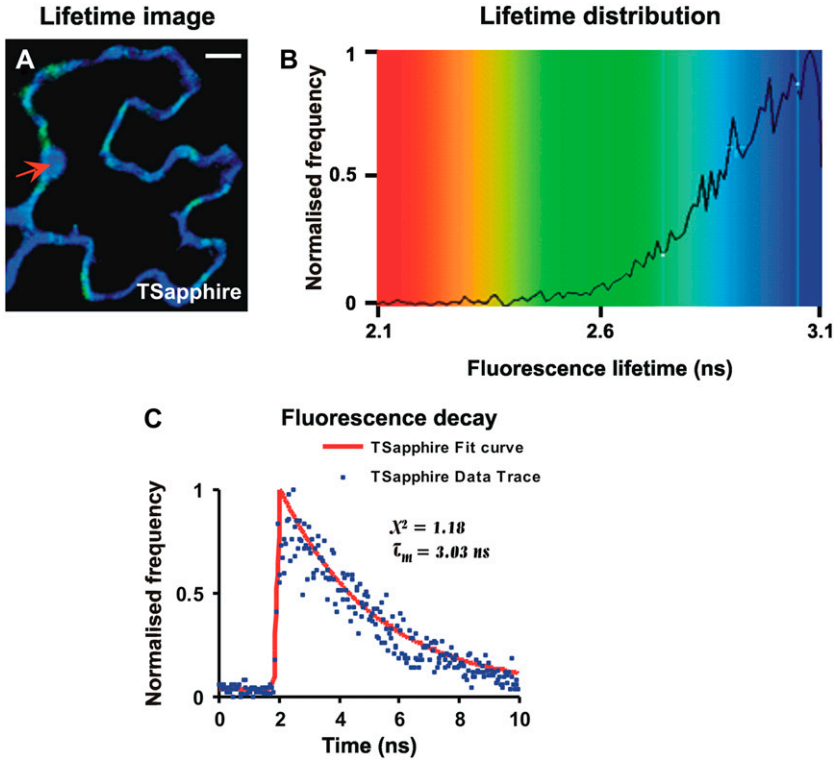

Figure 2. Excited-state lifetime analysis of TSapphire expressed in *N. benthamiana* cells. A, Time-correlated single photon fluorescence lifetime image of TSapphire. Scale bar = 25 μm. B, Overall lifetime profile of all the pixels in A. The false color code in A and B depicts the lifetime window from 2.1 ns (red) to 3.1 ns (blue). C, Unfitted data trace, single exponential fitted fluorescence decay curve, χ^2 fit, and lifetime (T_m) of a selected region (red arrowhead) in A.

Figure 3E shows that the fitted curve around the 3 × 3 pixel region (red arrowhead) in Figure 3C decays faster than the fitted curve around a similar region (red arrowhead) in Figure 3A. To corroborate the energy transfer from TSapphire to mOrange, we used FRET-acceptor photobleaching (FRET-APB) as an independent and complimentary method to our FRET-FLIM assay (see Supplemental Materials and Methods S1 and Supplemental Fig. S1). Bleaching of the acceptor mOrange in living cells expressing chimeric TSapphire-mOrange fusion protein resulted in dequenching of the donor TSapphire, whereas no such dequenching of TSapphire was observed following bleaching of mOrange in the cells expressing free TSapphire and mOrange (Supplemental Fig. S1). The calculated mean FRET-APB efficiencies were 12.28% for cells expressing chimeric TSapphire-mOrange and 0.52% for cells coexpressing free TSapphire and mOrange (Supplemental Fig. S1, columns M and N).

TSapphire-mOrange Donor-Acceptor Pair Reports on Intermolecular Interactions

Having confirmed the intramolecular FRET between TSapphire and mOrange, we next tested whether the TSapphire and mOrange pair could successfully and reliably report on the intermolecular interactions using the FRET-FLIM. For this purpose, we fused the donor and acceptor to some known biochemical and/or genetic interactors. The interactions were tested between (1) Arabidopsis (*Arabidopsis thaliana*) cytosolic proteins (RAR1 and SGT1b) that are known to be involved in *R* gene-mediated plant defense against pathogens and have been shown to interact genetically and biochemically (Azevedo et al., 2002); (2) maize (*Zea mays*)-specific plant transcriptional activator Opaque2 (O2) and transcriptional adaptor ADA2, a coactivator protein that may directly interact with transcriptional activators to modulate the transcription of downstream gene products (Bhat et al., 2004); and (3) barley (*Hordeum*

Table I. *Averaged mean lifetimes and calculated FRET-FLIM efficiencies of the donor TSapphire in the presence and absence of the acceptor mOrange in in planta intra- and intermolecular protein-protein interactions*

Proteins	Average Lifetimes	*n*	FRET Efficiency
	ns		%
TSapphire	2.93 ± 0.09	10	
TSapphire + mOrange	2.87 ± 0.08	12	2%
TSapphire-mOrange	2.48 ± 0.04	10	15%
SGT1b-TSapphire	2.94 ± 0.04	8	
SGT1b-TSapphire + RAR1-mOrange	2.6 ± 0.19	8	12%
O2-TSapphire	2.95 ± 0.02	10	
O2-TSapphire + ADA2-mOrange	2.77 ± 0.03	10	6%
CaM-TSapphire	2.98 ± 0.11	14	
CaM-TSapphire + MLO-mOrange	2.71 ± 0.13	10	9%
TSapphire + MLO-mOrange	2.92 ± 0.07	8	2%

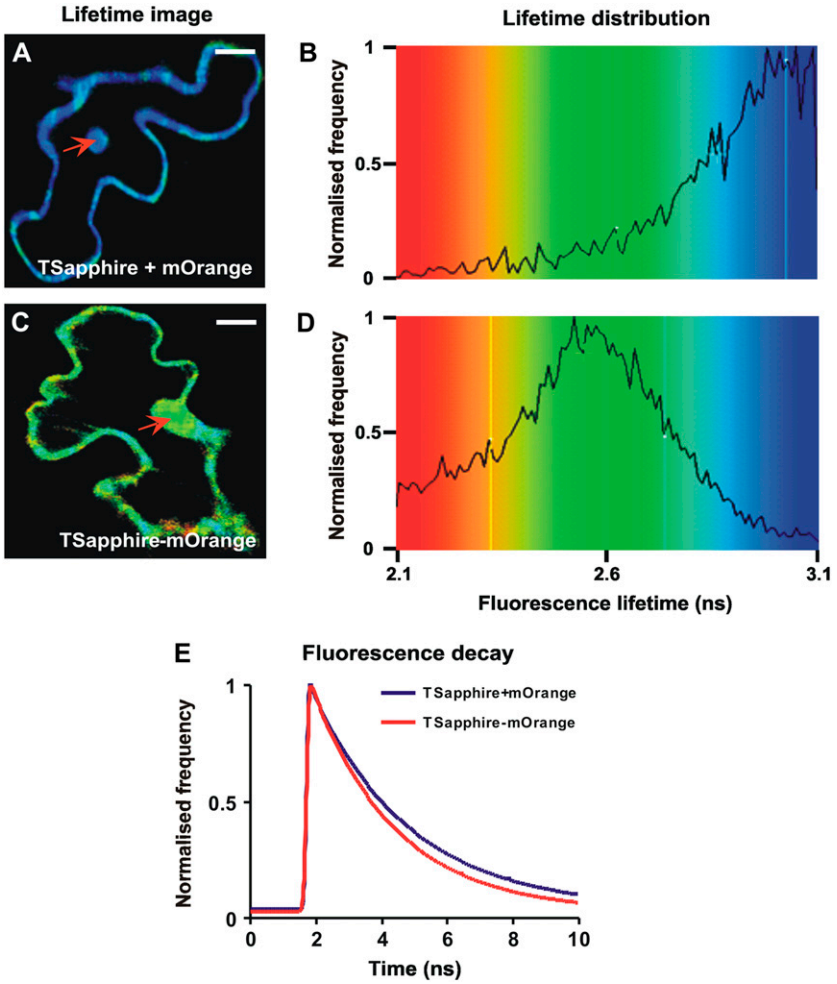

Figure 3. TSapphire + mOrange and TSapphire-mOrange FRET-FLIM in intact plant cells. A and C, Lifetime images of TSapphire in a cell coexpressing either TSapphire and mOrange (A) or chimeric TSapphire-mOrange (C). B and D, Overall lifetime profile of all the pixels in A and C, respectively. E, Fitted fluorescence decay curve of a selected region (red arrowhead) in A and C. The false color code in A to D depicts the lifetime of TSapphire from 2.1 ns (red; strong interaction) to 3.1 ns (blue; no interaction). Scale bars = 20 μm.

vulgare) integral membrane protein MLO and the cytosolic calcium sensor protein calmodulin (CaM), which are involved in defense against powdery mildew fungus (*Blumeria graminis*) and have been shown to interact genetically as well as via cell biological methods (Kim et al., 2002; Bhat et al., 2005).

We selected the above protein pairs for testing our TSapphire/mOrange FRET-FLIM system because this presented us with the possibility of not only testing interactions in different subcellular compartments (cytosol, nucleus, and at cellular periphery) but also to assess the nature of these interactions (stable versus dynamic interactions as discussed below).

RAR1 and SGT1b proteins fused to TSapphire and/or mOrange, expressed in *N. benthamiana* leaves colocalized in the cytosol (Supplemental Fig. S2). We found that the two proteins interact with each other in the cytosol regardless of whether SGT1b or RAR1 is fused to the donor TSapphire (Fig. 4). However, unlike the chimeric TSapphire-mOrange (Fig. 3C), the lifetime reduction was not observed throughout the cell but was restricted to certain peculiar locations (Fig. 4, C and H). This resulted in a mosaic pattern where, at some locations, TSapphire decayed with longer lifetimes (blue color in Fig. 4, C and H), indicating an absence of acceptor in the vicinity, whereas at other locations there was a dramatic reduction in the lifetime characteristic of resonance energy transfer (warmer colors in Fig. 4, C and H). One likely explanation for this would be that in the chimeric construct, TSapphire and mOrange are linked by a 16-amino acid linker and thus always stay at a fixed distance, resulting in a continuous FRET, whereas, in the case of RAR1 and SGT1b, the interaction and hence FRET are dynamic in nature. Fitted decay curves in Figure 4, E and J, from regions showing the color changes in Figure 4, C and H, respectively, confirmed that the photons in these regions decay much faster than the photons in similar-sized regions from Figure 4, A or F. Despite the nonuniformity of lifetime decay, the overall FRET-FLIM efficiency for the energy transfer from SGT1b-TSapphire to RAR1-mOrange in three independent experiments was found to be 12% (Table I). Similar FRET-FLIM efficiencies were obtained when the donor and acceptor fluorophores were swapped between SGT1b and RAR1 (data not shown).

The coexpression of nuclear-encoded maize transcriptional activator O2 and the coactivator ADA2 fused to TSapphire and mOrange, respectively (Sup-

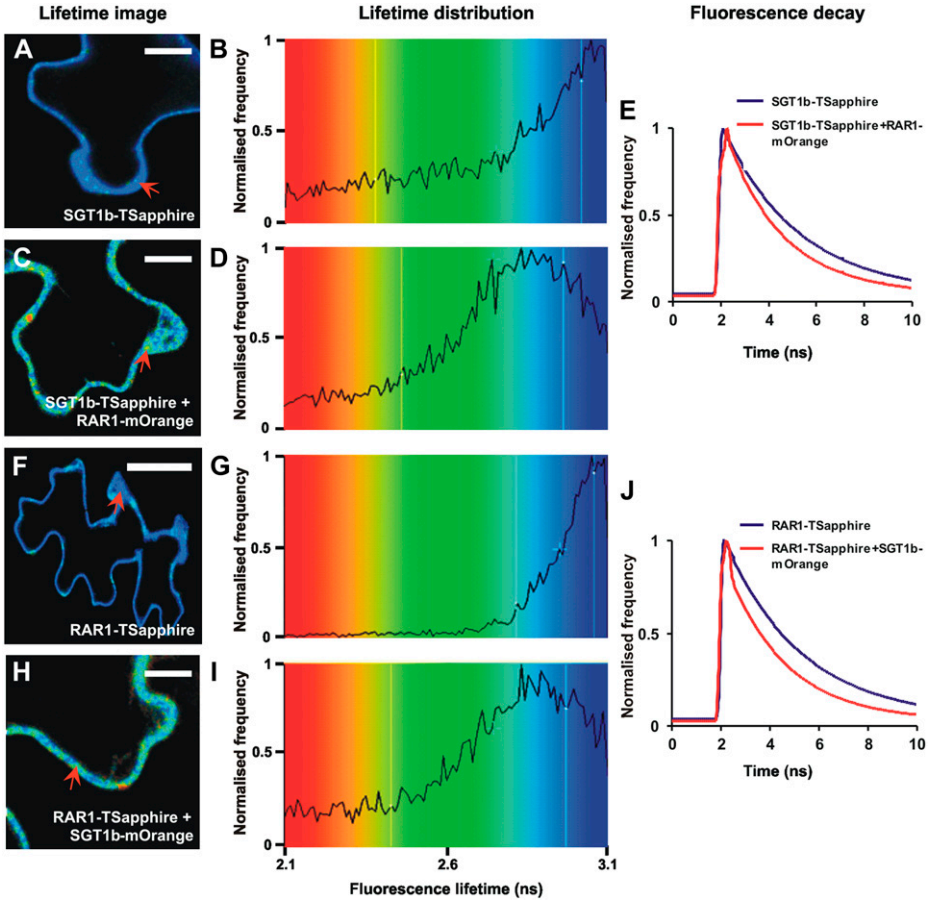

Figure 4. FRET-FLIM analysis on two Arabidopsis cytosolic proteins, SGT1 and RAR1, expressed in *N. benthamiana* cells. Lifetime image along with overall lifetime distribution profile of TSapphire in a cell expressing SGT1b-TSapphire alone (A and B), SGT1b-TSapphire and RAR1-mOrange (C and D), RAR1-TSapphire alone (F and G), or RAR1-TSapphire and SGT1b-mOrange (H and I). E, Comparison between fitted decay curves of a selected region (red arrowheads) in A and C, whereas J depicts the same for the selected regions in F and H. The false color code in A to I (excluding E) depicts the lifetime of the donor TSapphire from 2.1 ns (red color; strong interaction) to 3.1 (blue color; no interaction). Scale bars = 15 μm, except for F, where it is 45 μm.

plemental Fig. S3), resulted in a small but reproducible shift in the lifetime of the donor from 2.95 ± 0.02 ns for O2-TSapphire alone to 2.77 ± 0.03 ns for O2-TSapphire in the presence of ADA2-mOrange (Table I) that amounts to a FRET-FLIM efficiency of around 6%. Figure 5, A to H, shows the lifetime images and the overall lifetime distribution profiles of representative nuclei coexpressing free TSapphire and mOrange (Fig. 5, A and B), O2-TSapphire alone (Fig. 5, C and D), O2-TSapphire and ADA2-mOrange (Fig. 5, E and F), or ADA2-TSapphire and O2-mOrange (Fig. 5, G and H). Like the pattern observed in Figure 4, C and H, the lifetime reduction was observed in a nonuniform way, possibly pointing toward the dynamic nature of these protein-protein interactions. Figure 5I compares the fitted decay curve of a 3 × 3 pixel region (red arrowhead) from Figure 5, A, C, E, and G. Clearly the decay is much faster in situations where TSapphire fused to either O2 or ADA2 is in the presence of the acceptor mOrange fused to ADA2 or O2, respectively.

As a final confirmation of the reliability of the FRET-FLIM based on the TSapphire and mOrange donor-acceptor FRET pair, we tested interaction between the integral membrane protein MLO and the cytosolic calcium sensor protein CaM from barley in our transient single-cell FRET-FLIM assay in *N. benthamiana* leaves (Supplemental Fig. S4). Genetic and physical interaction between MLO and CaM was recently shown to modulate the entry of powdery mildew fungi into barley leaf epidermal cells (Kim et al., 2002; Bhat et al., 2005). In accordance with published data, we found that the two proteins interact with each other (Fig. 6, C–F versus A and B) and there is a reduction in the lifetime of CaM-TSapphire (from 2.98 ± 0.11 ns to 2.71 ± 0.13 ns) when expressed together with MLO-mOrange that results in a FRET-FLIM efficiency of around 9%. Such a lifetime reduction is absent in control cells coexpressing free TSapphire and MLO-mOrange (Fig. 6, G and H; Table I). As shown in Figure 6I, a sample fitted decay curve from Figure 6, C and E, decays much faster than sample decay curves from Figure 6, A and G.

DISCUSSION

Among many commonly used fluorescence-based methods including bioluminescence resonance energy transfer (Xu et al., 2007) and bimolecular fluorescence complementation (Magliery and Regan, 2006), FRET has emerged as a powerful tool to study in vivo protein dynamics and associations. One of the most direct and robust ways to assess FRET is by recording the excited-state lifetime changes in the donor fluorophore in the

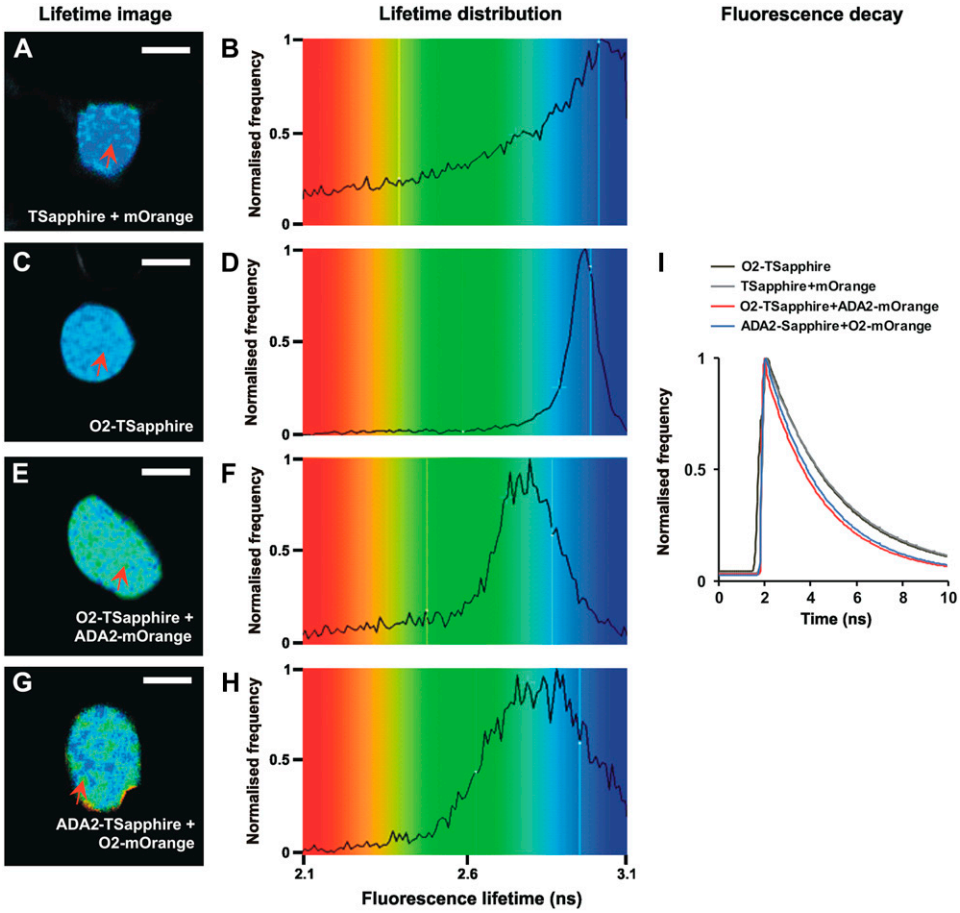

Figure 5. FRET-FLIM analysis on nuclear-encoded maize transcriptional activator O2 and transcriptional coactivator ADA2. Lifetime image along with overall lifetime distribution profile of TSapphire in the nucleus of representative cells coexpressing TSapphire and mOrange (A and B), O2-Tsapphire (C and D), O2-TSapphire and ADA2-mOrange (E and F), or ADA2-TSapphire and O2-mOrange (G and H). I, Comparison between fitted decay curves of a selected region (red arrowheads) from A and C against a similar region from E and G. The false color code in A to H depicts the lifetime of the donor TSapphire from 2.1 ns (red color; strong interaction) to 3.1 (blue color; no interaction). Scale bars = 5 μm.

absence and presence of an acceptor using FLIM (Gadella et al., 1999; van Munster and Gadella, 2005). FRET measurements using FLIM are superior to other methods (like intensity-based sensitized FRET or APB) because fluorescence lifetimes are independent of local chromophore concentrations and moderate photobleaching (Gadella et al., 1999; Immink et al., 2002; Bhat et al., 2006).

In this article, we demonstrate that the combination of TSapphire and mOrange as a donor-acceptor FRET-FLIM pair successfully reports on the intra- and intermolecular protein interactions. TSapphire as a donor is superior to current favorite CFP in many respects. First, the extinction coefficient (ε) and QY of TSapphire ($\varepsilon = 44{,}000\ \text{M}^{-1}\ \text{cm}^{-1}$; QY = 0.6) are far better than that of CFP (ε = 26,000 $\text{M}^{-1}\ \text{cm}^{-1}$; QY = 0.4; Patterson et al., 2001; Zapata-Hommer and Griesbeck, 2003) and thus much lower amounts of energy are needed to excite TSapphire. Second, fluorophores like blue fluorescent protein and CFP that emit in the blue range are more prone to photobleaching than GFP or TSapphire that emit in the green range (Gadella et al., 1999; Dixit et al., 2006). Furthermore, the optimal excitation of TSapphire with a 405-nm diode laser virtually leads to no excitation of the acceptor mOrange. Last, unlike CFP, TSapphire (like its parent GFP) exhibits monoexponential decay kinetics (shown in this study) and thus any lifetime reduction seen in TSapphire in the close presence of mOrange is more likely to be due to FRET.

Whereas any of the red-shifted monomeric proteins, like mStrawberry or mCherry, can be used as acceptors with TSapphire, we chose mOrange because it is the brightest red-shifted monomer (Shaner et al., 2005) and its emission spectrum does not overlap with that of chlorophyll autofluorescence. However, the spectral overlap necessary for efficient energy transfer from the donor to the acceptor is less extensive between TSapphire and mOrange compared to that between CFP and YFP (Gadella et al., 1999; Zapata-Hommer and Griesbeck, 2003; Shaner et al., 2004), and this might lead to lower measured FRET efficiencies. On the other hand, there is almost no spectral bleed through from TSapphire into mOrange (Zapata-Hommer and Griesbeck, 2003; Shaner et al., 2004, 2005). This is expected to result in more reliable FRET efficiencies while using any of the documented FRET methodologies. Photobleaching of mOrange, although a disadvantage in normal fluorescence imaging, can be used to advantage in the APB method for FRET measurement (Karpova et al., 2003; Bhat et al., 2006) to monitor changes in the donor fluorescence intensity following APB. If rapid photobleaching of mOrange is the main concern and FRET-FLIM is the sole method to be used for assessing the molecular associations, then TSapphire can be paired with recently described mOrange2, which

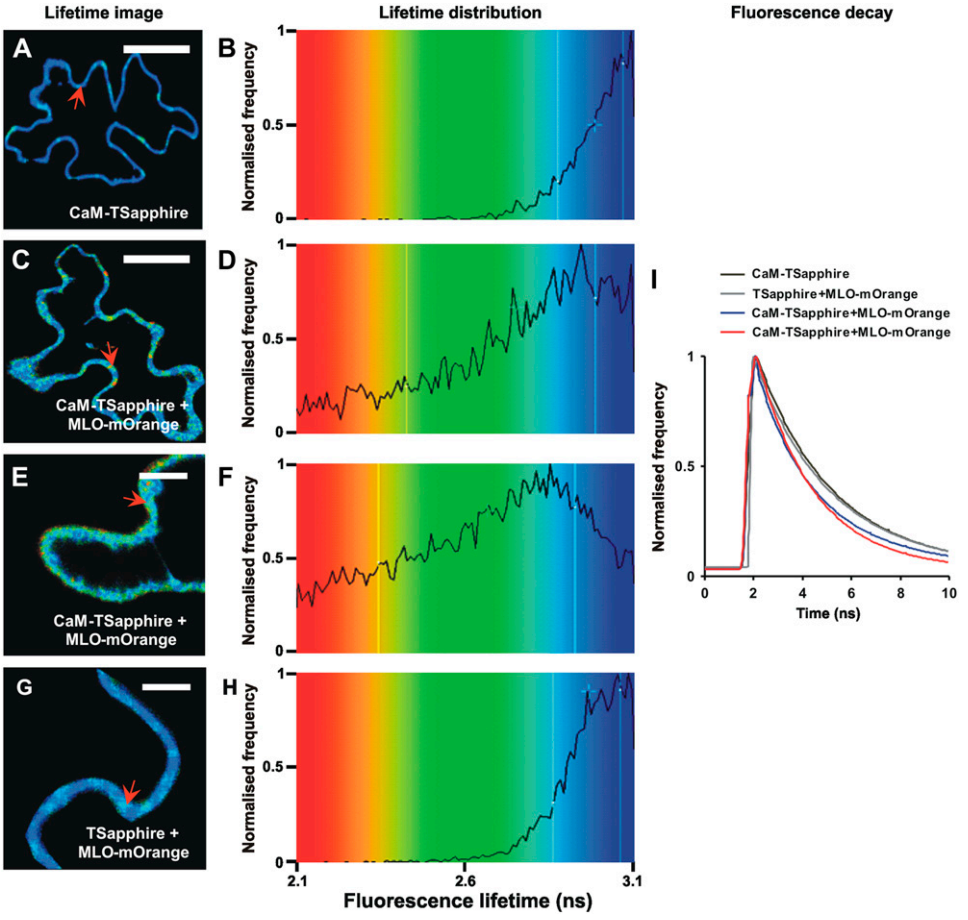

Figure 6. FRET-FLIM analysis on integral membrane protein MLO and cytosolic barley CaM. Lifetime image along with the overall lifetime distribution profile of representative cells expressing CaM-TSapphire alone (A and B), CaM-TSapphire and MLO-mOrange (C to F), or TSapphire and MLO-mOrange (G and H). I, Comparison between fitted decay curves of a selected region (red arrowheads) in A, C, E, and G. The false color code in A to H depicts the lifetime of the donor from 2.1 ns (red color; strong interaction) to 3.1 (blue color; no interaction). Scale bars = 45 μm for A and B; 15 μm for E and G.

has been shown to be 25-fold more photostable than the parent mOrange (Kremers and Piston, 2008).

To make a standard for in planta FRET-FLIM measurements, we took advantage of Gateway cloning technology (Invitrogen) and recombined TSapphire into a Gateway-compatible entry clone harboring mOrange (see "Materials and Methods"). This resulted in a chimeric construct where TSapphire was separated from mOrange by a 16-amino acid linker. FRET-FLIM analysis on this construct in *N. benthamiana* resulted in a mean FRET efficiency of 15%. Similar FRET efficiencies (12.28%) were obtained using the FRET-APB method for documenting energy transfer (Supplemental Fig. S1), thus corroborating the results obtained by FRET-FLIM. However, our calculated FRET efficiencies are reduced compared to a chimeric construct between Cerulean C1 (CFP variant) and Venus C1 (YFP variant), which exhibited 38% of FRET efficiency in HEK293 cells (Koushik et al., 2006). The comparatively reduced FRET efficiency could arise from the inherent properties of TSapphire and mOrange besides a number of properties of the unoptomized chimera. First, the spectral overlap between TSapphire and mOrange is less extensive than the overlap for Cerulean and Venus, so we expect less efficient transfer based solely on the photophysical properties of the protein set. Second, the 16-amino acid Gateway recombination linker (KGGRADPAFLYKVVDG) separating TSapphire from mOrange contains several structural amino acids (e.g. Pro, Phe) that may restrict the alignment of chromophore dipole moments required for FRET, even if the proteins are in close enough proximity for FRET. Despite these lower intramolecular FRET-FLIM efficiencies, we obtained reproducible intermolecular FRET-FLIM efficiencies confirming the nanometer scale closeness and hence molecular association between RAR1/SGT1b, ADA2/O2, and MLO/CaM protein pairs. Whereas the interaction between ADA2/O2 and MLO/CaM was recently shown using CFP-YFP as a donor acceptor FRET pair (Bhat et al., 2004, 2005), this report demonstrates an interaction between Arabidopsis RAR1 and SGT1b using in vivo cell biological methods. Thus, combining the distinct advantages of both TSapphire and mOrange, we provide data demonstrating interaction between diverse plant proteins expressed in different subcellular compartments in intact plant cells.

This study reports on the interaction between different plant proteins in various subcellular compartments under a single set of conditions and criteria demonstrating, therefore, the versatility of the system proposed here. Furthermore, we have developed a set of Gateway technology-compatible plant-specific vectors

that can be used by the interested researchers for studying their protein pairs of interest to facilitate the use of this system. Thus, it is our contention that this study should serve as a reference point for researchers attempting to set up the TSapphire-mOrange donor-acceptor FRET-FLIM in planta.

MATERIALS AND METHODS

Plasmids

The backbone of all the vectors used in the study was pam-PAT-MCS (accession no. AY436765). To generate fluorescent protein destination vectors for Gateway cloning technology (Invitrogen), PCR-amplified TSapphire (Zapata-Hommer and Griesbeck, 2003) and mOrange (Shaner et al., 2004) were inserted into the pXCS-HisHA vector containing 2× the cauliflower mosaic virus constitutive 35S promoter (Witte et al., 2004), resulting in p35S::TSapphire-nos and p35S::mOrange-nos. A Gateway recombination cassette was ligated into p35S::TSapphire-nos and p35S::mOrange-nos, and the resulting clones, p35S::GW-TSapphire-nos and p35S-GW-mOrange-nos, were selected. The cDNA sequences of Arabidopsis (*Arabidopsis thaliana*) RAR1 (L. Noel and J. Parker, unpublished data) and SGT1b (Witte et al., 2004), maize (*Zea mays*) GCN5 and O2 (Bhat et al., 2003, 2004), and barley (*Hordeum vulgare*) MLO and CaM (Kim et al., 2002; Bhat et al., 2005) cloned into entry vectors (pENTR or pENTR/D-TOPO from Invitrogen) were recombined into p35S::GW-TSapphire-nos and p35S::GW-mOrange-nos. For the TSapphire-mOrange chimeric fusion protein, the TSapphire cDNA cloned into pENTR/D-TOPO was recombined into the destination vector p35S::GW-mOrange-nos to yield the p35S::TSapphire-mOrange-nos chimeric construct. A 16-amino acid linker (KGGRADPAFLYKVVDG) separated the two fluorophores after recombination. All the clones were verified by sequencing.

Plant Material and Transient Single-Cell Gene Expression

Nicotiana benthamiana was cultivated in the greenhouse as described (Romeis et al., 2001). Detached leaves from 5- to 6-week-old plants were placed into petri dishes containing 1% agar and the transient gene expression in the epidermal cells mediated by particle bombardment was performed as described (Bhat et al., 2005). For colocalization and FRET-FLIM, equimolar amounts of plasmids were coated onto the gold particles. After bombardment, leaves were incubated for 18 to 48 h at room temperature prior to microscopic analysis.

CLSM

Transient intracellular fluorescence was observed by CLSM using a Leica SP2 AOBS inverted confocal microscope (Leica Microsystems) equipped with argon ion (458-, 476-, 488-, 496-, and 514-nm laser lines) and the He-Ne (561-nm laser line) lasers. Additionally, a 405-nm diode laser (BDL 405 SMC; Becker and Hickl) operating either in continuous or pulsing mode was also installed into the Leica SP2 AOBS system. TSapphire was excited with a 405-nm diode laser running in continuous mode, whereas mOrange was excited with a 514-nm (and occasionally 561) argon laser line. TSapphire fluorescence was detected using the Leica AOBS system and a custom 485- to 535-nm band-pass emission filter, whereas mOrange fluorescence was detected using the Leica AOBS system and a custom 545- to 600-nm band-pass emission filter. For spectroscopic analysis, the emission spectra of TSapphire and mOrange were collected in the λ-spectral mode between 450 to 590 nm for TSapphire and 540 to 720 nm for mOrange. Reference spectra of TSapphire, mOrange, and chlorophyll autofluorescence were used to linearly unmix the relevant spectra and subtract any chlorophyll background. A 63× HCX PLAN-APO Water immersible objective lens (N.A. = 1.2; ref. 506212; Leica) was used for imaging bombarded cells.

TCSPC-FLIM Data Acquisition

FLIM analysis was performed using the TCSPC (with SPC 830 card) system from Becker and Hickl (Becker et al., 2004) fitted into the SP2 AOBS via the X1 port of the Leica SP2 AOBS microscope. The data were acquired according to the manufacturer's recommendations (Leica D-FLIM; http://www.becker-hickl.de/leicaman.htm). To excite the donor TSapphire, a 405-nm diode laser pulsing at 80 MHz was used and data acquisition was done for 4 min in 40 cycles (6 s/cycle). TSapphire emission was selected via a 520DF40-nm band-pass filter (Chroma). Images were collected in 512 × 512 pixel mode. *N. benthamiana* cells are very big and contain a large central vacuole that pushes the cytoplasm and the nucleus to the cell periphery and results in poor count rates in TCSPC-FLIM imaging. Thus, to increase the count rates/pixel and hence the resolution, only selected magnified areas of the cells were subjected to FLIM analysis. However, whenever possible, the whole cells were used for data collection and analysis.

FLIM Data Analysis

The lifetime data acquired using the TCSPC system were imported into SPC image software (version 2.9; Becker and Hickl) and analyzed using the default conditions (scatter, shift, and decay components unfixed). The complete lifetime decays were calculated per pixel as per the χ^2 goodness-of-fit rule (described below) and fitted by using the monoexponential decay model for cells expressing TSapphire alone and with the double exponential decay model for cells expressing TSapphire along with mOrange. Only pixels with more than 30 to 50 photons were used for building the lifetime profile. To get a better signal-to-noise ratio in decay curves, the pixels were generally binned by a factor of 2 or 3. The raw data containing lifetime information per pixel were exported into Microsoft Excel and average lifetime values along with standard deviations were obtained. Experiments were repeated at least three times to get statistically valid data. The efficiency of energy transfer (E) based on the fluorescence lifetime (τ) was calculated as $E = 1 - (\tau_{D+A}/\tau_{D-A})$, where τ_{D+A} is donor fluorescence lifetime in the presence of acceptor while τ_{D-A} is the donor fluorescence lifetime in the absence of acceptor (Bastiaens and Squire, 1999; Gadella et al., 1999).

χ^2 Goodness-of-Fit Rule

To estimate fluorescence lifetimes, an accurate mathematical representation of the fluorescence decay data is crucial. Several assumptions are made to fit the fluorescence decay curves. The goodness-of-fit parameter χ^2, as well as the residuals generated for a given fit, measures how well the fitted curve represents the actual data (Koushik et al., 2006). χ^2 values closer to 1.0 yield better fits than the ones away from it. Data were fitted as per the criteria set by Koushik et al. (2006). Essentially, data were first fit to a single exponential decay model and χ^2 value was noted. Subsequently, a double exponential decay model was applied to the same dataset. If the χ^2 value of the double exponential decay model fitted curve was ≤ one-half of the χ^2 value generated by a single exponential model fit, the double exponential model was accepted (Koushik et al., 2006).

Supplemental Data

The following materials are available in the online version of this article.

Supplemental Figure S1. FRET-APB analysis on TSapphire + mOrange and TSapphire-mOrange in intact plant cells.

Supplemental Figure S2. Coexpression of Arabidopsis SGT1b and RAR1 fused to TSapphire and mOrange in intact plant cells.

Supplemental Figure S3. Coexpression of maize O2 and ADA2 fused to TSapphire and mOrange in intact plant cells.

Supplemental Figure S4. Coexpression of barley CaM and MLO fused to TSapphire and mOrange in intact plant cells.

Supplemental Materials and Methods S1. FRET-APB.

ACKNOWLEDGMENTS

We thank Dr. Oliver Griesbeck (Max Planck Institute of Neurobiology Am Klopferspitz, Martinsried, Germany) and Prof. Roger Tsien (Howard Hughes Medical Institute, University of California, San Diego) for the kind donation of cDNA clones encoding TSapphire and mOrange, respectively. Dr. Wendy A. Peer (Purdue University, West Lafayette, IN) is kindly acknowledged for help with APB experiments. The FRET-APB work performed by Dr. Peer was funded by a U.S. Department of Agriculture grant to Roberto Gaxiola and

Angus Murphy at Purdue University. We also wish to thank Dr. Laurent Noël (LIPM-INRA/CNRS, Castanet, France) and Dr. Sidney Shaw (Indiana University, Bloomington, IN) for criticism, suggestions, and helpful comments.

Received February 5, 2008; accepted July 5, 2008; published July 11, 2008.

LITERATURE CITED

Azevedo C, Sadanandom A, Kitagawa K, Freialdenhoven A, Shirasu K, Schulze-Lefert P (2002) The RAR1 interactor SGT1, an essential component of R gene-triggered disease resistance. Science **295:** 2073–2076

Bastiaens PI, Squire A (1999) Fluorescence lifetime imaging microscopy: spatial resolution of biochemical processes in the cell. Trends Cell Biol **9:** 48–52

Becker W, Bergmann A, Haustein E, Petrasek Z, Schwille P, Biskup C, Kelbauskas L, Benndorf K, Klocker N, Anhut T, et al (2006) Fluorescence lifetime images and correlation spectra obtained by multidimensional time-correlated single photon counting. Microsc Res Tech **69:** 186–195

Becker W, Bergmann A, Hink MA, Konig K, Benndorf K, Biskup C (2004) Fluorescence lifetime imaging by time-correlated single-photon counting. Microsc Res Tech **63:** 58–66

Bhat RA, Borst JW, Riehl M, Thompson RD (2004) Interaction of maize Opaque-2 and the transcriptional co-activators GCN5 and ADA2, in the modulation of transcriptional activity. Plant Mol Biol **55:** 239–252

Bhat RA, Lahaye T, Panstruga R (2006) The visible touch: in planta visualization of protein-protein interactions by fluorophore-based methods. Plant Methods **2:** 12

Bhat RA, Miklis M, Schmelzer E, Schulze-Lefert P, Panstruga R (2005) Recruitment and interaction dynamics of plant penetration resistance components in a plasma membrane microdomain. Proc Natl Acad Sci USA **102:** 3135–3140

Bhat RA, Riehl M, Santandrea G, Velasco R, Slocombe S, Donn G, Steinbiss HH, Thompson RD, Becker HA (2003) Alteration of GCN5 levels in maize reveals dynamic responses to manipulating histone acetylation. Plant J **33:** 455–469

Chapman S, Oparka KJ, Roberts AG (2005) New tools for in vivo fluorescence tagging. Curr Opin Plant Biol **8:** 565–573

Dixit R, Cyr R, Gilroy S (2006) Using intrinsically fluorescent proteins for plant cell imaging. Plant J **45:** 599–615

Fricker M, Runions J, Moore I (2006) Quantitative fluorescence microscopy: from art to science. Annu Rev Plant Biol **57:** 79–107

Gadella TW Jr, van der Krogt GN, Bisseling T (1999) GFP-based FRET microscopy in living plant cells. Trends Plant Sci **4:** 287–291

Immink RG, Gadella TW Jr, Ferrario S, Busscher M, Angenent GC (2002) Analysis of MADS box protein-protein interactions in living plant cells. Proc Natl Acad Sci USA **99:** 2416–2421

Jares-Erijman EA, Jovin TM (2003) FRET imaging. Nat Biotechnol **21:** 1387–1395

Karpova TS, Baumann CT, He L, Wu X, Grammer A, Lipsky P, Hager GL, McNally JG (2003) Fluorescence resonance energy transfer from cyan to yellow fluorescent protein detected by acceptor photobleaching using confocal microscopy and a single laser. J Microsc **209:** 56–70

Kim MC, Panstruga R, Elliott C, Muller J, Devoto A, Yoon HW, Park HC, Cho MJ, Schulze-Lefert P (2002) Calmodulin interacts with MLO protein to regulate defence against mildew in barley. Nature **416:** 447–451

Koushik SV, Chen H, Thaler C, Puhl HL III, Vogel SS (2006) Cerulean, Venus, and VenusY67C FRET reference standards. Biophys J **91:** L99–L101

Kremers GJ, Piston DW (2008) Turning fluorescent proteins into energy-saving light bulbs. Nat Methods **5:** 472–473

Magliery TJ, Regan L (2006) Reassembled GFP: detecting protein-protein interactions and protein expression patterns. Methods Biochem Anal **47:** 391–405

Patterson G, Day RN, Piston D (2001) Fluorescent protein spectra. J Cell Sci **114:** 837–838

Romeis T, Ludwig AA, Martin R, Jones JD (2001) Calcium-dependent protein kinases play an essential role in a plant defence response. EMBO J **20:** 5556–5567

Shah K, Gadella TW Jr, van Erp H, Hecht V, de Vries SC (2001) Subcellular localization and oligomerization of the Arabidopsis thaliana somatic embryogenesis receptor kinase 1 protein. J Mol Biol **309:** 641–655

Shaner NC, Campbell RE, Steinbach PA, Giepmans BN, Palmer AE, Tsien RY (2004) Improved monomeric red, orange and yellow fluorescent proteins derived from Discosoma sp. red fluorescent protein. Nat Biotechnol **22:** 1567–1572

Shaner NC, Steinbach PA, Tsien RY (2005) A guide to choosing fluorescent proteins. Nat Methods **2:** 905–909

Striker G, Subramaniam V, Seidel CAM, Volkmer A (1999) Photochromicity and fluorescence lifetimes of green fluorescent protein. J Phys Chem B **103:** 8612–8617

Tramier M, Gautier I, Piolot T, Ravalet S, Kemnitz K, Coppey J, Durieux C, Mignotte V, Coppey-Moisan M (2002) Picosecond-hetero-FRET microscopy to probe protein-protein interactions in live cells. Biophys J **83:** 3570–3577

Tsien RY (1998) The green fluorescent protein. Annu Rev Biochem **67:** 509–544

van Munster EB, Gadella TW (2005) Fluorescence lifetime imaging microscopy (FLIM). Adv Biochem Eng Biotechnol **95:** 143–175

Volkmer A, Subramaniam V, Birch DJ, Jovin TM (2000) One- and two-photon excited fluorescence lifetimes and anisotropy decays of green fluorescent proteins. Biophys J **78:** 1589–1598

Witte CP, Noel LD, Gielbert J, Parker JE, Romeis T (2004) Rapid one-step protein purification from plant material using the eight-amino acid StrepII epitope. Plant Mol Biol **55:** 135–147

Xu X, Soutto M, Xie Q, Servick S, Subramanian C, von Arnim AG, Johnson CH (2007) Imaging protein interactions with bioluminescence resonance energy transfer (BRET) in plant and mammalian cells and tissues. Proc Natl Acad Sci USA **104:** 10264–10269

Zapata-Hommer O, Griesbeck O (2003) Efficiently folding and circularly permuted variants of the Sapphire mutant of GFP. BMC Biotechnol **3:** 5